NINETEENTH EUROPEAN ROTORCRAFT FORUM

Paper n° G7

A MULTILEVEL DECOMPOSITION PROCEDURE FOR EFFICIENT DESIGN OPTIMIZATION OF HELICOPTER ROTOR BLADES

by

Aditi Chattopadhyay, Thomas R. McCarthy and Narayanan Pagaldipti

Department of Mechanical and Aerospace Engineering
Arizona State University
Tempe, Arizona 85287-6106

September 14-16, 1993
CERNOBBIO (Como)
ITALY

ASSOCIAZIONE INDUSTRIE AEROSPAZIALI
ASSOCIAZIONE ITALIANA DI AERONAUTICA ED ASTRONAUTICA

A MULTILEVEL DECOMPOSITION PROCEDURE FOR EFFICIENT DESIGN OPTIMIZATION OF HELICOPTER ROTOR BLADES

Aditi Chattopadhyay†, Thomas R. McCarthy‡ and Narayanan Pagaldipti‡
Department of Mechanical and Aerospace Engineering
Arizona State University
Tempe, Arizona 85287-6106

1. Abstract

This paper addresses a multilevel decomposition procedure, for efficient design optimization of helicopter blades, with the coupling of aerodynamics, blade dynamics, aeroelasticity and structures. The multidisciplinary optimization problem is decomposed into three levels. The rotor is optimized for improved aerodynamic performance at the first level. At the second level, the objective is to improve the dynamic and aeroelastic characteristics of the rotor with a constraint on the autorotational inertia. In the third level, the goal is to design a two celled isotropic box beam for minimum blade weight while ensuring that the blade structure maintains sufficient stiffness. Nonlinear chord and twist distributions are assumed. Interdisciplinary coupling is established through the use of optimal sensitivity derivatives. The Kreisselmeier Steinhauser function approach is used to formulate the optimization problem when multiple design objectives are involved. A nonlinear programming technique and an approximate analysis procedure are used for optimization. Results obtained show significant improvements in the rotor aerodynamic, dynamic and structural characteristics, when compared to a reference or baseline rotor.

2. Nomenclature

c	chord, ft
c_0 - c_3	chord distribution parameters, ft
f_r	3/rev radial shear, lb
f_x	3/rev inplane shear, lb
f_z	4/rev vertical shear, lb
f	K-S function constraint vector
g	constraint functions
m_c	3/rev torsional moment, lb-ft
m_x	3/rev flapping moment, lb-ft
m_z	4/rev lagging moment, lb-ft
w_{oj}	nonstructural weight at j^{th} node, lb
x, y, z	reference axes
$\bar{y}$	nondimensional radial location
AI	autorotational inertia, lb-ft^2
C_T	thrust coefficient
C_P	power coefficient
EI_{xx}	lagging stiffness, lb-ft^2
EI_{zz}	flapping stiffness, lb-ft^2
F_k	objective functions
F_{ko}	values of F_k at the beginning of an iteration
K	total number of constraints and objective functions
NC	number of constraints
NDV	number of design variables
NOBJ	number of objective functions
NSEG	number of blade segments
NMEM	number of box beam structural members

† Assistant Professor, Senior Member AIAA, Member AHS, ASME, SPIE
‡ Graduate Research Assistant, Member AHS, AIAA

R	blade radius, ft
T	thrust, lb
W	total blade weight, lb
α_j	real part of the j^{th} stability root
ϵ_k	k^{th} objective function tolerance
ϕ	design variable vector
μ	advance ratio
ρ	K-S function multiplier
θ	blade twist, degrees
θ_1 - θ_3	blade twist parameters, degrees
σ	area-weighted solidity
σ_r	blade root centrifugal stress, lb/ft^2
υ_j	minimum allowable damping of j^{th} stability root
Ω	rotor angular velocity, r.p.m.

3. Introduction

In recent years, optimization techniques have received wide attention in helicopter rotor blade design for addressing various design issues involving dynamics, aerodynamics, structures and aeroelasticity. Considerable research on aeroelastic optimization of metal rotor blades has been performed during the last decade as indicated by Friedmann [1]. Chattopadhyay and Walsh [2] addressed vibration reduction and minimum weight design of rotor blades with stress constraints. Recently, Chopra and Ganguli [3] developed an aeroelastic optimization and sensitivity analysis procedure for composite hingeless rotors using an analytical approach. Most of these research efforts were based on a single discipline.

Rotary wing aircraft design is truly multidisciplinary in nature and therefore an integration of the necessary disciplines is essential for an optimization procedure to be meaningful. Celi and Friedmann [4] addressed the coupling of dynamic and aeroelastic criteria, using quasi steady airloads, for blades with straight and swept tips. An integrated aerodynamic and dynamic optimization procedure was presented by Chattopadhyay et. al. [5]. The integration of aerodynamic loads and dynamics was achieved by coupling the comprehensive helicopter analysis code CAMRAD [6] with the optimization algorithm CONMIN [7] and an approximate analysis technique. He and Peters [8] performed a combined structural, dynamic and aerodynamic optimization of rotor blades using a simple box beam model to represent the structural component in the blade. Chattopadhyay and McCarthy [9,10] developed multicriteria optimization procedures for the design of helicopter rotor blades. The objectives were to reduce blade vibration with the coupling of blade dynamics, aerodynamics, aeroelasticity and structures. Very recently, multidisciplinary optimization efforts have also been initiated to investigate the design of high speed proprotors by Chattopadhyay et. al. [11,12].

Since the validity of the designs obtained using optimization techniques depends strongly upon the accuracy of the analysis procedures used, it is essential to integrate sufficiently comprehensive analysis tools within the closed loop optimization procedure. Such procedures are C.P.U. intensive and, hence, are computationally prohibitive in an optimization environment. Furthermore, since the problem becomes highly coupled and is associated with a large number of design variables, an "all-at-once" optimization procedure in which all the disciplines are coupled and optimization is performed based on criteria involving every discipline, can be inefficient and time consuming. Therefore, decomposition techniques are often used to simplify such complex optimization problems into a number of sub problems. Multilevel decomposition techniques have been applied to problems involving a single discipline [13-16] and are finding applications in multidisciplinary design optimization of fixed wing aircraft [17-20]. In this paper, such a procedure is used to address the complex helicopter rotor blade design problem. Typically, the number of levels is based on the number of disciplines involved. Individual optimization is performed at each level using analysis procedures pertaining to that level. Optimal sensitivity parameters are exchanged between the levels to provide the necessary coupling between the levels. An optimal design is obtained when each individual level is converged and overall convergence is achieved. Therefore, the speed of obtaining a fully converged result depends upon the strength of coupling between the various levels. A smart

decomposition procedure enables systematic decomposition in which the coupling between the levels are minimal. The following section presents a simple decomposition scheme for a generic problem.

4. Multilevel Decomposition

The multilevel decomposition procedure is illustrated through a three-level formulation. Each level is a multiobjective optimization problem characterized by a vector of objective functions, constraints and design variables. The formulation is outlined below.

LEVEL 1

$$\text{Minimize} \quad F_i^1(\phi_1) \qquad i = 1, \ldots, NOBJ^1$$

$$\text{subject to} \quad g_k^1(\phi_1) \leq 0 \qquad k = 1, \ldots, NC^1$$

$$\sum_{i=1}^{NDV^1} \frac{\partial F_j^{2^*}}{\partial \phi_i^1} \Delta\phi_i^1 \leq \varepsilon_j^2 \qquad j = 1, \ldots, NOBJ^2$$

$$\sum_{i=1}^{NDV^1} \frac{\partial F_j^{3^*}}{\partial \phi_i^1} \Delta\phi_i^1 \leq \varepsilon_j^3 \qquad j = 1, \ldots, NOBJ^3$$

$$\phi_i^{1L} \leq \phi_i^1 \leq \phi_i^{1U} \qquad i = 1, \ldots, NDV^1$$

$$\phi_j^{2L} \leq \phi_j^{2^*} + \sum_{i=1}^{NDV^1} \frac{\partial \phi_j^{2^*}}{\partial \phi_i^1} \Delta\phi_i^1 \leq \phi_j^{2U} \qquad j = 1, \ldots, NDV^2$$

$$\phi_j^{3L} \leq \phi_j^{3^*} + \sum_{i=1}^{NDV^1} \frac{\partial \phi_j^{3^*}}{\partial \phi_i^1} \Delta\phi_i^1 \leq \phi_j^{3U} \qquad j = 1, \ldots, NDV^3$$

where F^1, F^2 and F^3 are the objective function vectors at levels 1, 2 and 3 respectively, g^1, g^2 and g^3 are the corresponding constraint vectors and ϕ^1, ϕ^2 and ϕ^3 are the corresponding design variable vectors. The quantities ε_j^2 and ε_j^3 represent tolerances on the changes in the j^{th} objective functions corresponding to levels 2 and 3, respectively. Superscripts L and U refer to lower and upper bounds, respectively and superscript * represents optimum values. The quantities, $\frac{\partial F_j^{2^*}}{\partial \phi_i^1}$ and $\frac{\partial F_j^{3^*}}{\partial \phi_i^1}$ are the optimal sensitivity derivatives of the objective functions used at levels 2 and 3, respectively, with respect to the design variables at level 1. Finally, $\frac{\partial \phi_j^{2^*}}{\partial \phi_i^1}$ and $\frac{\partial \phi_j^{3^*}}{\partial \phi_i^1}$ are the optimal sensitivity derivatives of the design variables vectors at levels 2 and 3, respectively, with respect to the design variables at level 1.

LEVEL 2

$$\text{Minimize} \quad F_j^2(\phi^{1^*}, \phi^2) \qquad j = 1, \ldots, NOBJ^2$$

$$\text{subject to} \quad g_k^2(\phi^{1^*}, \phi^2) \leq 0 \qquad k = 1, \ldots, NC^2$$

$$\sum_{i=1}^{NDV2} \frac{\partial F_j^{3^*}}{\partial \phi_i^2} \Delta\phi_i^2 \le \varepsilon_j^3 \qquad j = 1, ..., NOBJ^3$$

$$\phi_i^{2L} \le \phi_i^2 \le \phi_i^{2U} \qquad i = 1, ..., NDV^2$$

$$\phi_j^{3L} \le \phi_j^{3^*} + \sum_{i=1}^{NDV^2} \frac{\partial \phi_j^{3^*}}{\partial \phi_i^2} \Delta\phi_i^2 \le \phi_j^{3U} \qquad j = 1, ..., NDV^3$$

where ϕ^{1*} is the optimum design variable vector from level 1. This vector is kept fixed during optimization at level 2. The optimal sensitivity derivatives of the level 3 objective functions and design variables with respect to level 2 design variables are denoted $\frac{\partial F_j^{3^*}}{\partial \phi_i^2}$ and $\frac{\partial \phi_j^{3^*}}{\partial \phi_i^2}$, respectively.

Level 3

Minimize	$F_j^3(\phi^{1^*}, \phi^{2^*}, \phi^3)$	$j = 1, ..., NOBJ^3$
subject to	$g_k^3(\phi^{1^*}, \phi^{2^*}, \phi^3)$	$k = 1, ..., NC^3$
	$\phi_j^{3L} \le \phi_j^3 \le \phi_j^{3U}$	$j = 1, ..., NDV^3$

where the optimum vectors from upper levels, ϕ^{1*} and ϕ^{2*}, are held constant. Iterations between the three levels are necessary to account for the coupling between the objective functions, constraints and design variables pertaining to the various levels.

5. Problem Formulation

The decomposition of the helicopter rotor blade optimization problem is described here. As mentioned earlier, a smart decomposition can decouple the problem efficiently and help achieve faster convergence. This can be accomplished through a knowledge of the design process and synthesis as well as the magnitudes of the optimal sensitivity derivatives. In the conventional design process of an aircraft, the planform variables are prescribed by the aerodynamicist. The desired stiffnesses of the wing are prescribed by the dynamicist and the structural engineer designs the wing structure with sufficient stiffnesses. Based on the above concept, coupled with a knowledge of the optimal sensitivity parameters, the rotor design problem is decomposed into three levels.

Level 1

The rotor is optimized for improved aerodynamic performance at level 1 of the procedure. The total power coefficient, C_P, is the objective function. Level 1 design variables include spanwise variations of chord and twist distributions. A constraint is imposed on the rotor thrust coefficient, C_T, to ensure the same lifting capability of the reference rotor. In order not to deviate too much from the baseline flight condition and also to ensure efficiency in hover a lower bound is imposed on the rotor solidity, σ. The constraints are formulated as follows

(i) $C_T = C_{Tref}$,

(ii) $\sigma \ge \sigma_{min}$,

where the subscript "ref" stands for the reference, or baseline, rotor and the subscript "min" refers to the minimum allowable blade solidity.

Level 2

At level 2, the objective is to improve the dynamic and aeroelastic characteristics of the rotor and control the vibratory and static stresses on the blade. For a four-bladed rotor in forward flight, the most critical vibratory hub loads occur at the fundamental blade passing frequency of 4/rev. This also includes contributions from the 3/rev and 5/rev loads as well [21]. However, the magnitudes of the 5/rev loads are small compared to the 3/rev loads and are therefore ignored. The six critical vibratory loads are the 4/rev vertical shear (f_z), the 4/rev lagging moment (m_z), the 3/rev inplane shear (f_x), the 3/rev radial shear (f_r), the 3/rev flapping moment (m_x) and 3/rev torsional moment (m_c). In this problem, the 4/rev vertical shear, f_z, and the 3/rev inplane shear, f_x, are included as objective functions since their values were found to be more significant. A constraint is imposed on the 3/rev radial force, f_r. The moments are not included to reduce the number of constraints. A lower bound is imposed on the autorotational inertia (AI) to ensure that the rotor has sufficient inertia to autorotate in the event of engine failure. Constraints are also imposed on the real part of the stability roots to maintain aeroelastic stability. These constraints assume the following form,

$$\text{(iii)} \quad f_r \le f_{rU},$$
$$\text{(iv)} \quad AI \ge AI_L,$$
$$\text{(v)} \quad \alpha_k \le -\upsilon, \qquad k = 1, 2, \ldots, K,$$

where f_{rU} is the upper bound on the radial shear and the subscript AI_L is the lower bound on the autorotational inertia. The quantity α_k represents the real part of the stability root, K denotes the total number of modes included and υ denotes a minimum allowable blade damping which is a positive number.

The design variables used in level 2 are discrete values of the flapping and lagging stiffnesses, EI_{zz_i} and EI_{xx_i}, respectively, at each segment (i = 1, ... , NSEG and NSEG is the total number of blade segments). Discrete values of the nonstructural weights (Fig. 1) located at the blade tip, w_{o_i}, (i = 1, ... , NSEG) are also used as design variables.

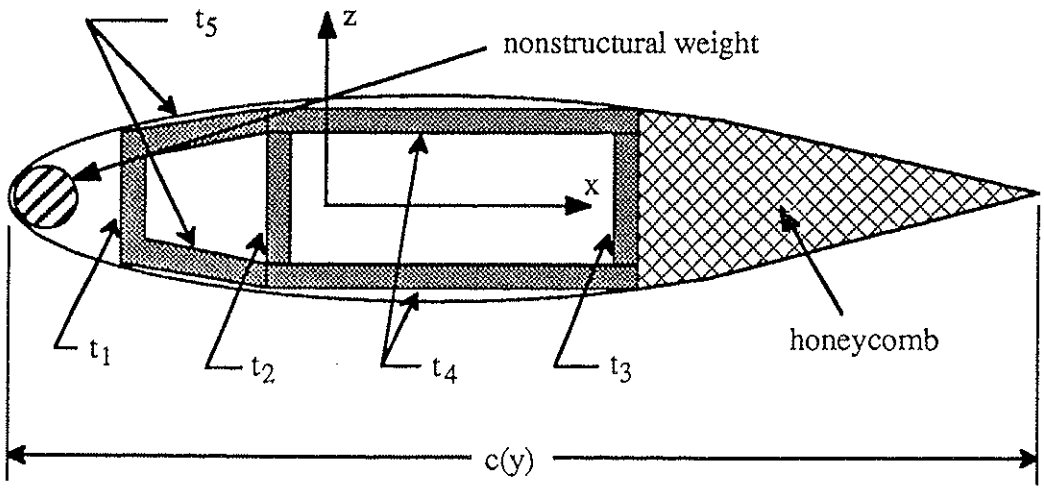

Fig. 1 Two celled isotropic box beam

Level 3

At level 3, it is of interest to design the spar such that optimum structural stiffnesses from level 2 match the actual stiffnesses of the box beam. The appropriate objective function is the total blade weight which is to be minimized. The five independent wall thicknesses (Fig. 1), at each section t_{j_i} (j = 1, ... , 5, Fig. 1), are used as design variables.

To ensure that the actual flapping and lagging stiffnesses are close to the optimum stiffnesses, as determined in level 2, these stiffnesses are constrained to be within a small tolerance of the optimum stiffnesses. An upper bound constraint (σ_{max}) is imposed on the blade centrifugal stress, at the root, σ_r. The constraints are as follows.

$$\text{(vi)} \quad |EI_{xx} - EI_{xx_{opt}}| \le \varepsilon(EI_{xx_{opt}})$$

(vii) $|EI_{zz} - EI_{zz_{opt}}| \leq \varepsilon(EI_{zz_{opt}})$

(viii) $\sigma_r \leq FS \times \sigma_{max}$

where $EI_{xx_{opt}}$ and $EI_{zz_{opt}}$ are the optimum stiffnesses obtained from level 2, ε is the allowable tolerance on the deviations, FS is the factor of safety and σ_{max} is the maximum allowable blade stress.

6. Aerodynamic Model

The rotor blade aerodynamic model is described in this section. The blade chord and twist distributions are modeled as nonlinear functions of the nondimensionalized radius, $\bar{y}$. The chord, $c(\bar{y})$, and twist distributions, $\theta(\bar{y})$, are defined to have the following spanwise variations.

$$c(\bar{y}) = c_0 + c_1(\bar{y} - .75) + c_2(\bar{y} - .75)^2 + c_3(\bar{y} - .75)^3 \quad (1)$$

$$\theta(\bar{y}) = \theta_1(\bar{y} - .75) + \theta_2(\bar{y} - .75)^2 + \theta_3(\bar{y} - .75)^3 \quad (2)$$

where the coefficients c_0 - c_3 and θ_1 - θ_3 are the coefficients that define the chord and twist shapes, respectively. These distributions are chosen to closely model the properties of an existing blade [22]. The nonlinear distributions also allow the optimizer sufficient flexibility in the design space, since these parameters are used as design variables.

7. Structural Model

The load carrying structural member in the rotor is modeled as a two cell isotropic box beam (Fig. 1) with five independent wall thicknesses which are assumed to vary spanwise. Spanwise nonstructural tuning masses are located at 2.5 percent chord location. The beam is symmetrical about the x-axis and is assumed to carry all loads within the rotor. Outer dimensions of the box beam at a blade section are based on constant percentages of the chord at that particular section. Titanium is used as the blade material.

Since the flapping and lagging stiffnesses are used as design variables in level 2, the remaining structural properties, as required by the code CAMRAD, are estimated based on these values. For example, the polar moment of inertia (I_θ), the torsional rigidity (GJ), the shear center - center of gravity offset (x_i) and the blade mass (m) are estimated based upon the current values of the flapping and lagging stiffnesses and the values of the respective stiffnesses from the last real analysis. All other physical blade properties are assumed to remain constant. From these values it is then possible to estimate the total blade weight (W), the autorotational inertia (AI) and the centrifugal stress at the root (σ_r)

8. Multiobjective Function Formulation

Due to the fact that the optimization problem in level 2 involves more than one design objective, the Kreisselmeier-Steinhauser (K-S) function approach [23] is used. Using this approach, the problem with multiple objective functions and constraints is transformed into one with a composite function which comprises properly scaled objective functions and constraints. The optimization problem is reduced to an unconstrained minimization of the K-S function. The K-S function approach has been found to perform well in the nonlinear helicopter design problem [10]. The original objective functions are transformed into reduced objective functions which assume the following form.

$$F_k^*(\phi) = \frac{F_k(\phi)}{F_{k_0}} - 1 - g_{max} \leq 0 \qquad K = 1, 2, \ldots, NOBJ, \quad (3)$$

where F_{k_0} represents the value of the original objective function, F_k, calculated at the beginning of each iteration. The quantity g_{max} is the value of the largest constraint corresponding to the design variable vector ϕ and is held constant during each iteration. These reduced objective functions are

analogous to the previous constraints. Therefore, a new constraint vector $g_m(\phi)$, m = 1, 2, ... , M, is introduced, where M = NC + NOBJ. This constraint vector includes the original constraints of the problem as well as the constraints introduced through Eqn. 3. The new objective function is defined as follows.

$$\tilde{F}(\Phi) = f_{max} + \frac{1}{\rho}\sum_{m=1}^{M} e^{\rho(g_m(\Phi)-f_{max})}, \qquad (4)$$

where f_{max} is the largest constraint corresponding to the new constraint vector, $g_m(\phi)$, and in general is not equal to g_{max}. The K-S multiplier ρ is analogous to a draw-down factor where ρ controls the distance from the surface of the K-S objective function to the surface of the maximum constraint function. When ρ is large, the K-S function closely follows the surface of the largest constraint function. When ρ is small, the K-S function includes contributions from all violated constraints. The design variable vector ϕ remains unchanged using this multiobjective function formulation technique. Further details are found in Ref. [10].

9. Analysis and Optimization

The program CAMRAD is used for the blade dynamic, aerodynamic and aeroelastic stability analyses. The code uses lifting line theory, with corrections for yawed flow, to calculate the section loading based on the two-dimensional aerodynamic characteristics of the airfoil. At each cycle of the optimization procedure the blade is trimmed within CAMRAD so that the intermediate designs which represent feasible designs are trimmed configurations. A wind tunnel trim option is used and the rotor lift and drag, each normalized with respect to solidity and the flapping angle are trimmed using the collective pitch, the cyclic pitch and the shaft angle. Uniform inflow is assumed to reduce computational effort.

The optimized rotor is trimmed to the same value of the thrust coefficient (C_T) as the reference rotor using a variable trim procedure [10]. The blade response is calculated, in CAMRAD, using rotating free-vibration modes equivalent to a Galerkin analysis. Ten bending modes, of which seven are flapping dominated and three are lead-lag dominated, and three torsion modes are calculated. Main blade responses of up to 8/rev are included. Therefore, eight harmonics of the rotor revolution are retained in the airloads calculations. The vibratory shear forces and moments are calculated based upon the airloads information obtained from the aerodynamic analysis. The aeroelastic stability analysis is performed using Floquet theory for periodic state equations. Four bending degrees of freedom and one torsional degree of freedom are used for the stability analysis.

The structural analysis of the rotor blade is performed using an in-house code [24]. The blade section properties are based on thin wall theory. The code models a simple two cell homogeneous box beam with one rectangular cell and one trapezoidal cell (Fig. 1). It is assumed that the flatwise, chordwise and torsional stiffnesses of the blade are provided solely by the box beam.

The optimization algorithm used is CONMIN which is a nonlinear programming technique based upon the method of feasible directions. Since the use of exact analyses for the calculations of the objective functions and constraints during each iteration within CONMIN is computationally prohibitive, an approximate analysis technique, based on a two-point exponential approximation [25] is used. This technique assumes its name from the fact that the exponent used in the expansion is based on gradient information from the previous design point. Further details of the expansion technique can be found in Refs. [10,25].

10. Results

The optimization procedure is applied to a reference blade of radius, R = 4.685 ft and rotational velocity, Ω = 639.5 r.p.m. which is operating in forward flight with an advance ratio, μ = 0.3. The rotor is an existing advanced four-bladed articulated rotor. The blade is discretized into 10 segments (NSEG = 10). A summary of the flight conditions is presented in Table 1. The physical constraints imposed during optimzation include the blade solidty (σ), the autorotational inertia (AI), the centrifugal stress at the blade root (σ_r), the minimum allowable blade damping (υ) and the 3/rev

inplane vibratory shear force (f_r). A value of $\sigma_{min} = 0.100$ is used as the lower bound on the solidity and the upper bound used on the autorotational inertia is 19.8 lb-ft^2 which is based on an existing advanced rotor blade value [22]. A minimum allowable blade damping of $\upsilon = 0.01$ is used to ensure that the optimum blade retains some damping. The reference value of $f_r = 1.11$lb is used as the upper bound on the 3/rev inplane shear force. The root centrifugal stress is constrained to be below 12.5 x 10^6 lb/ft^2, which is calculated using the allowable stress for titanium and a factor of safety, FS = 2. During the optimization procedure the constraints on the autorotational inertia and the centrifugal stress are always well satisfied, while the solidity becomes nearly active for the optimum blade. The 3/rev inplane shear force is reduced by 9.5 percent during the optimization procedure. Further details are seen in Table 2.

A total of 7 aerodynamic design variables are used in level 1 to define the chord and twist distributions. In level 2, 30 design variables are used to define the discrete spanwise variations of the flapping and lagging stiffnesses and the nonstructural weights. In level 3, the 5 individual wall thicknesses of the two celled isoptropic box beam lead to a total of 50 design variables along the span. Therefore, the entire multilevel decomposition optimization procedure consists of a total of 87 design varibles. Global convergence is achieved in only 3 cycles, requiring 14 total cycles in level 1, 45 cycles in level 2 and only 12 cycles in level 3.

Table 1 Summary of operating conditions

Blade radius, R	4.685 ft
Rotor thrust, T	277 lb
Rotational velocity, Ω	639.5 r.p.m.
Advance ratio, μ	0.3

The optimum results are presented in Tables 2 and 3 and Figs. 2 - 8. It is seen from Table 2 and Fig. 2 that there are significant reductions in the individual objective functions from all levels. The objective function in level 1, the coefficient of total power (C_P), is reduced by 19.8 percent. The 4/rev vertical shear (f_z), one of the objective functions in level 2, is reduced by 45.8 percent. The second objective function in level 2, the 3/rev inplane shear (f_x) remains equal to the reference value. The large reduction in f_z and no reduction in f_x is possibly due to the fact that the K-S function envelope follows the f_z surface more closely than f_x due to the value of the K-S factor, ρ, selected for this problem. It must also be noted that the procedure does not guarantee a global optimum, therefore the solution obtained represents a local minimum. The total blade weight (W), which is the objective function in level 3, is reduced by 3.7 percent. As shown in Table 2, the constraints for all three levels are well satisfied.

The chord and twist distributions, which are defined by level 1 design variables, are presented in Figs. 3 and 4. From Fig. 3 it is seen that optimum blade has a nearly linear tapered planform, despite the fact that the assumed chord distribution is cubic. As a consequence, the blade solidity is reduced from reference to optimum blade. This also implies that the optimum rotor is operating at a slightly higher C_T/σ value while maintaining the same rotor thrust as the reference rotor (Table 2). The optimum configuration is therefore tapered which represents a more aerodynamically efficient design with a more evenly distributed load distribution. The twist distribution is shown in Fig. 4 where significant changes are observed. The reference rotor has a linear twist distribution with nearly 16° of total twist, from root to tip. The optimum rotor has a highly nonlinear distribution and the total twist is significantly reduced (approximately 6°, from root to tip). The overall reduction is blade twist is possibly an attempt to minimize the region of negative angles of attack in the rotor map, thereby improving aerodynamic efficiency.

Table 2 Summary of optimum results

	Bounds lower	Bounds upper	Reference	Optimum
Objective Functions				
Level 1				
C_P			0.000470	0.000377
Level 2				
f_z (lb)			0.204	0.111
f_x (lb)			1.41	1.41
Level 3				
W (lb)			5.95	5.73
Constraints				
Level 1				
σ	0.100	-	0.116	0.104
Level 2				
f_r	-	1.11	1.11	1.00
AI (lb-ft^2)	19.8	-	39.4	33.9
Level 3				
σ_T (x 10^6 lb/ft^2)	-	12.5	1.51	1.51
Trim, C_T/σ			0.0592	0.0659

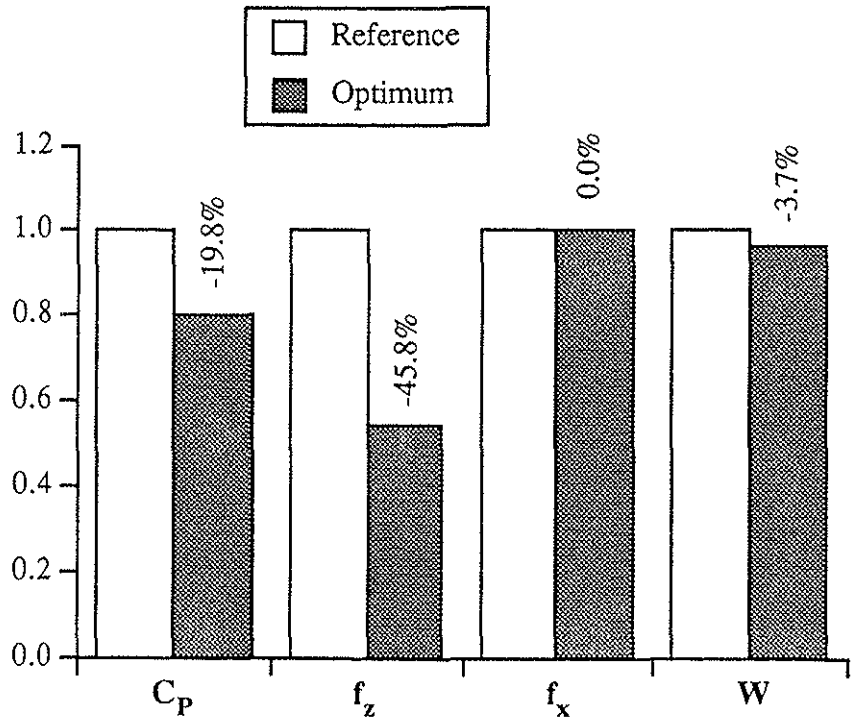

Fig. 2 Summary of optimum results

The level 2 design variables are shown in Figs. 5-7. Both the lagging stiffness (EI_{xx}) and the flapping stiffness (EI_{zz}) have similar trends. Due to the optimal sensitivity derivatives there is a very strong dependence of the stiffnesses on the chord distribution determined in level 1. This is due to the fact that as the chord changes, the dimensions of the box beam also change. Figure 5 depicts the lagging stiffness distribution where the similarities between the stiffness and chord distributions is observed. The nonlinearities in these distributions are possibly due to the optimizer's effort in altering the modes shapes (make them more orthogonal to the forcing function) to reduce vibration. The nonstructural weight (w_o) distributions are presented in Fig. 7. When compared to the reference

rotor, there is an increase in the magnitudes of these weights from root to 3/4 span followed by a subsequent decrease. This trend represents a compromise between the optimizer's effort in altering the dynamic response while reducing the blade weight. Although the autorotational inertia is used as a constraint, this constraint is always well satisfied and therefore does not influence the nonstructural weight distribution significantly.

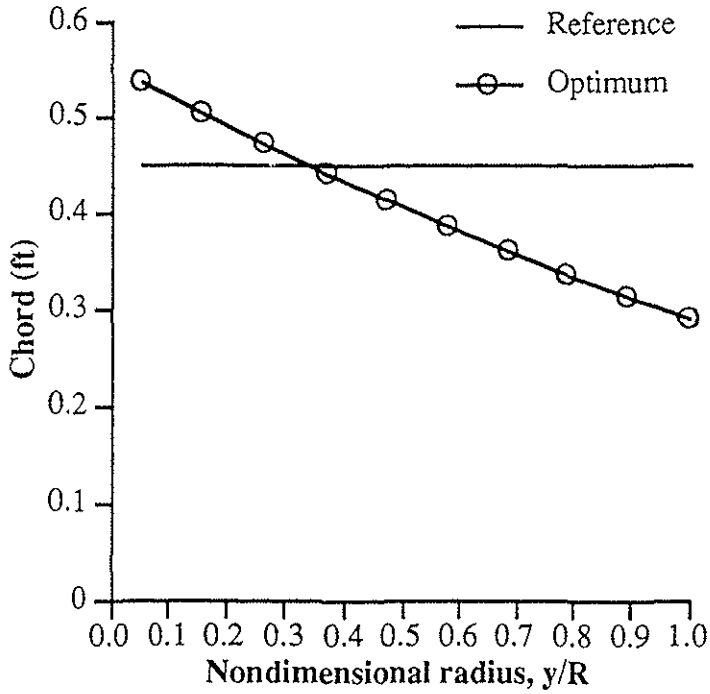

Fig. 3 Blade chord distributions

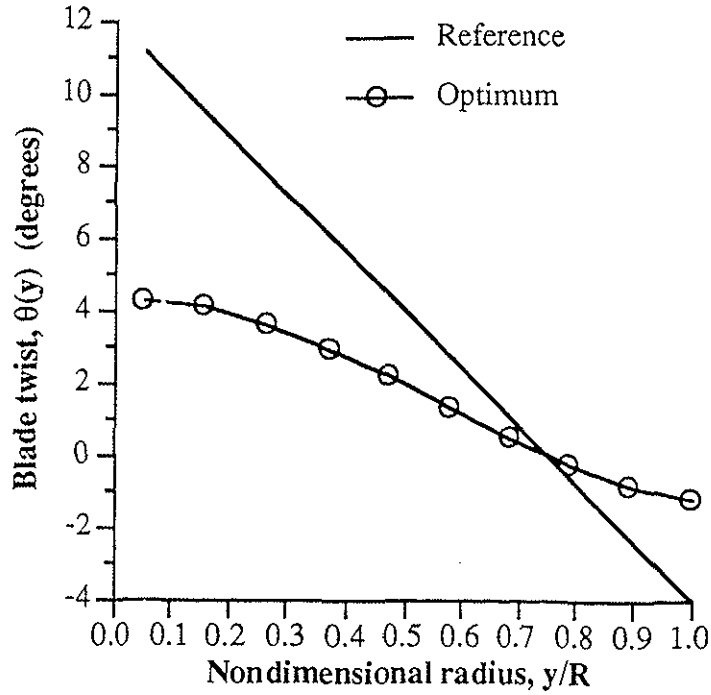

Fig. 4 Blade twist distributions

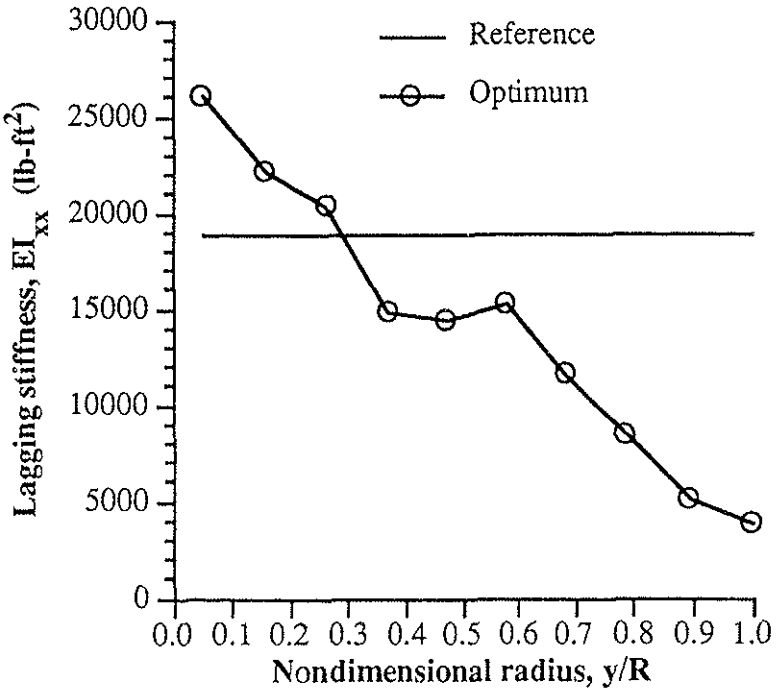

Fig. 5 Lagging stiffness distributions

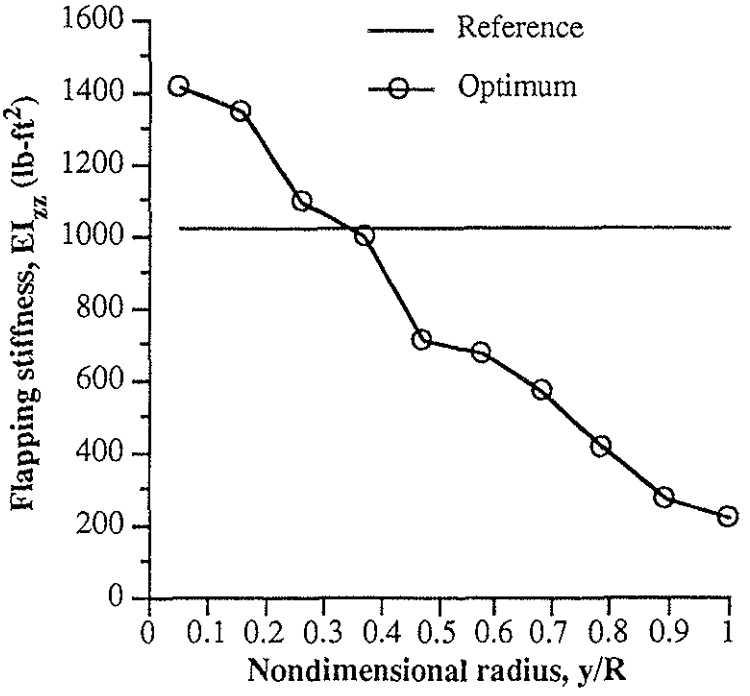

Fig. 6 Flapping stiffness distributions

The design variables of level 3 are presented in Table 3 which shows the discrete spanwise variance of the reference and optimum thicknesses for all five independent box beam wall thicknesses. The nonlinearities in the distributions are a result of the objective of level 3 which is to obtain a minimum weight structure that satisfies the stiffness distributions as predicted by level 2. Such a beam would be very impractical to build out of an isotropic material but the stiffness distributions can be easily achieved through composite tailoring.

Finally, Fig. 8 shows the root-locus diagram, which are level 2 constraints, for the optimum and reference rotors. It is seen that aeroelastic stability is maintained after optimization and that the blade has higher damping than the minimum prescribed value ($\upsilon = 0.01$).

Table 3 Box beam wall thicknesses

	Box Beam Wall Thicknesses (in)									
NSEG	1	2	3	4	5	6	7	8	9	10
Reference	0.0625	0.0625	0.0625	0.0625	0.0625	0.0625	0.0625	0.0625	0.0625	0.0625
t_1	0.0612	0.0613	0.0621	0.0601	0.0621	0.0648	0.0633	0.0631	0.0617	0.0636
t_2	0.0570	0.0495	0.0611	0.0431	0.0699	0.1105	0.0668	0.0670	0.0530	0.0453
t_3	0.0602	0.0551	0.0631	0.0469	0.0658	0.0820	0.0642	0.0657	0.0583	0.0636
t_4	0.0423	0.0585	0.0530	0.0825	0.0511	0.0693	0.0940	0.0766	0.0568	0.0749
t_5	0.0488	0.0422	0.0608	0.0290	0.0728	0.1032	0.0783	0.0711	0.0444	0.0225

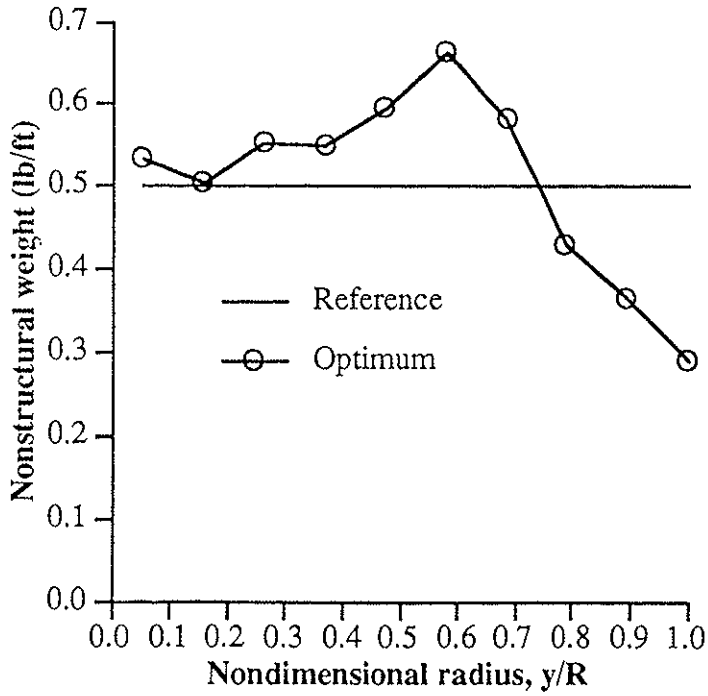

Fig. 7 Nonstructural weight distributions

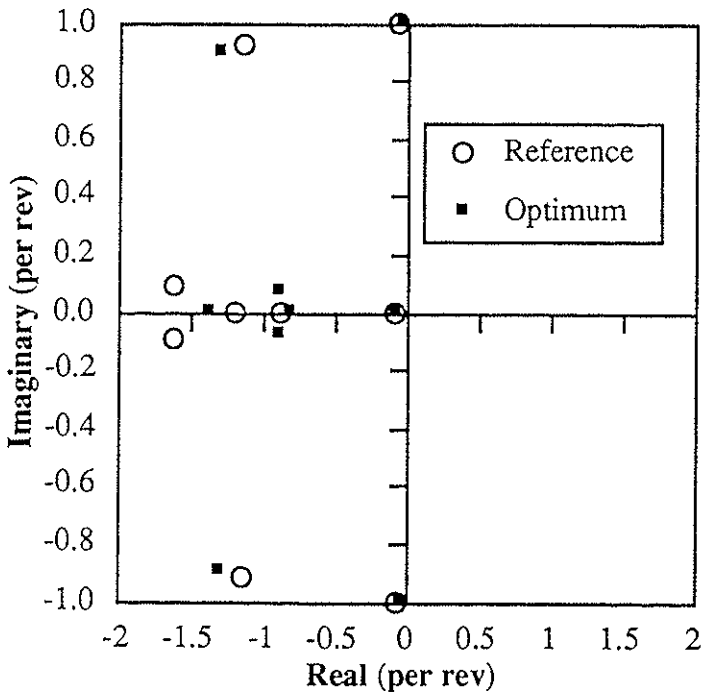

Fig 8 Root-locus diagram

In summary, the multilevel procedure developed is more efficient in formulating and addressing multidisciplinary design optimization of rotary wing aircraft. The decomposition helps in understanding the coupling between the various disciplinary criteria and the design variable linkage. The design objectives and constraints are all satisfied in the example shown. The procedure provides important design trends. Actual numbers obtained are somewhat less important as they should be viewed within the context of the modeling assumptions used in the analysis.

11. Concluding Remarks

A multilevel, multidisciplinary decomposition procedure has been developed for the optimal design of helicopter rotor blades. Blade aerodynamic, dynamic, aeroelastic and structural design requirements have been coupled within a three level decomposition optimization procedure. In level 1, the coefficient of total power is reduced using aerodynamic design variables. Level 2 comprises two objectives functions to be reduced, the 4/rev vertical shear and the 3/rev inplane shear. The two objective function problem is formulated using the Kreisselmeier-Steinhauser function approach. The design variables used are discrete spanwise distributions of the flapping and lagging stiffnesses and nonstructural weights. At level 3, the objective is to obtain a minimum weight spar design to satisfy the stiffnesses predicted by level 2. The design variables are discrete spanwise distributions of the 5 independent box beam wall thicknesses. A nonlinear programming approach is used in conjunction with a hybrid approximation technique. The procedure yields significant design improvements. The following specific observations are made within the context of the modeling assumptions used.

1. The multilevel decompostion optimization procedure yielded significant reductions in the objective functions in all three levels. The use of the decomposition technique allowed for more identifiable intrepretations of the results and its inclusion within the optimization procedure made the overall optimization problem more manageable.

2. The coefficient of total power was significantly reduced due to the more optimal chord and twist distributions obtained in level 1.

3. The stiffness and nonstructural weights distributions were altered to modify the mode shapes thereby reducing the blade vibration. The flapping and lagging stiffness distributions followed the chord distribution due to the use of optimal sensitivity derivatives, that linked the two levels.

4. The optimum rotor configuration remained aeroelastically stable throughout the optimization procedure even though stiffness and mass distributions were significantly altered.

12. References

1. Friedmann, P. P., "Helicopter Vibration Optimization using Structural Optimization with Aeroelastic/ Multidisciplinary Constraints," *Journal of Aircraft*, Vol. 28, No. 1, 1991, pp. 8-21.

2. Chattopadhyay, A., and Walsh, J. L., "Minimum Weight Design of Rotorcraft Blades with Multiple Frequency and Stress Constraints," *AIAA Journal*, Vol. 28, 3, 565-567, March 1990.

3. Ganguli, R. and Chopra, I., "Aeroelastic Optimization of a Helicopter Rotor with Composite Tailoring," *American Helicopter Society 49th Annual Forum*, St. Louis, Missouri, 1993.

4. Celi, R. and Friedmann, P. P., "Efficient Structural Optimization of Rotor Blades with Straight and Swept Tips," *Proceedings of the 13th European Rotorcraft Forum*, Arles, France, 1987.

5. Chattopadhyay, A., Walsh, J. L., and Riley, M. F., "Integrated Aerodynamic/Dynamic Optimization of Helicopter Blades," Special Issue of the *AIAA Journal of Aircraft on Multidisciplinary Optimization of Aeronautical Systems* , Vol. II, 58-65 January 1991.

6. Johnson, W., "A Comprehensive Analytical Model of Rotorcraft Aerodynamics and Dynamics," Part II: Users' Manual, NASA TM 81183, 1980.

7. Vanderplaats, G. N., "CONMIN - A FORTRAN Program for Constrained Function Minimization," Users' Manual, NASA TMX 62282, 1987.

8. He, C., and Peters, D. A., "Optimization of Rotor Blades for Combines Structural, Dynamic and Aerodynamic Properties," *Proceedings of the Third Airforce/ NASA Symposium on Recent Advances in Multidisciplinary Analysis and Optimization*, San Francisco, California, 1990.

9. Chattopadhyay, A., and McCarthy, T. R., "Recent Efforts at Multicriteria Design Optimization of Helicopter Rotor Blades," *Presented at the NATO/DFG ASI*, Berchtesgaden, Germany, September 1991.

10. Chattopadhyay, A., and McCarthy, T. R., "Multidisciplinary Optimization of Helicopter Rotor Blades Including Design Variable Sensitivity," *Engineering Composites*, Vol. 3, 1, 1993.

11. Chattopadhyay, A., and Narayan, J., "Optimum Design of High Speed Prop-Rotors Using a Multidisciplinary Approach," *48th Annual Forum of the American Helicopter Society*, Washington D. C., 1992. Also appearing in *Engineering Optimization* (in press).

12. Chattopadhyay, A., McCarthy, T. R. and Madden, J. F., "An Optimization Procedure for the Design of Prop-Rotors in High Speed Cruise Including the Coupling of Performance, Aeroelastic Stability and Structures," *Mathematical and Computer Modelling*, Special Issue on Rotorcraft, Vol. 17b, July 1993 (in press).

13. Schmit, L. A. and Merhinfar, M., "Multilevel Optimum Design of Structures with Fiber-Composite Stiffened-Panel Components," *AIAA Journal*, Vol. 20, No. 1, 1982, pp. 138-147.

14. Schmit, L. A. and Chang, K. J., "A Multilevel Method for Structural Synthesis," *25th AIAA/ASME/AHS/ASCE Structures, Structural Dynamics and Materials Conference*, Palm Springs, California, 1984.

15. Kirsch, U., "An Improved Multilevel Structural Synthesis Method," *Journal of Structural Mechanics*, Vol. 13, No. 2, 1985, pp. 123-144.

16. Sobieszczanski-Sobieski, J., James, B. B. and Riley, M. F., "Structural Optimization by Generalized, Multilevel Optimization," *26th AIAA/ASME/AHS/ASCE Structures, Structural Dynamics and Materials Conference*, Orlando, Florida, 1985.

17. Barthelemy, J. F. M., Wrenn, G. A., Dovi, A. R. and Coen, P. C., "Integrating Aerodynamics and Structures in the Minimum Weight Design of a Supersonic Transport Wing," *33rd AIAA/ASME/AHS/ASCE Structures, Structural Dynamics and Materials Conference*, Dallas, Texas, 1992.

18. Sobieszczanski-Sobieski, J., "Sensitivity Analysis and Multidisciplinary Optimization for Aircraft Design: Recent Advances and Results," NASA TM 100630 , 1988.

19. Barthelemy, J. F. M. and Riley, M. F., "Improved Multilevel Optimization Approach for the Design of Complex Engineering Systems," *AIAA Journal*, Vol. 26, No. 3, 1988, pp. 353-360.

20. Barthelemy, J. F. M., Coen, P. G., Wrenn, G. A., Riley, M. F., Dovi, A. R. and Hall, L.E., "Application of Multidisciplinary Optimization Methods to the Design of a Supersonic Transport," NASA TM-104073.

21. Gessow, A. and Myers, G.C., Aerodynamics of the Helicopter, College Park Press, 1985.

22. Chattopadhyay, A. and Chiu, Y. D., "An Enhanced Integrated Aerodynamic/Dynamic Approach to Optimum Rotor Blade Design," *Structural Optimization*, 4, 75-84, 1992.

23. Kreissemeier, A. and Steinhauser, R. "Systematci Control Design by Optimizing a Vector Performance Index," *Proceedings of the IFAC Symposium on Computer Aided Design of Control Systems*, Zurich, Switzerland, 1979, pp. 113-117.

24. McCarthy, T.R., An Integrated Multidisciplinary Optimization Approach For Rotary Wing Design, Master's Thesis, Arizona State University, December 1992.

25. Fadel, G. M., Riley, M. F. and Barthelemy, J. M., "Two Point Exponential Approximation Method for Structural Optimization," *Structural Optimization*, Vol. 2., pp. 117-224.